TYPE Original Research
PUBLISHED 21 February 2025
DOI 10.3389/fspas.2025.1513711

OPEN ACCESS

EDITED BY
Chuanfei Dong,
Boston University, United States

REVIEWED BY
Akos Kereszturi,
Hungarian Academy of Sciences (MTA), Hungary
James Head,
Brown University, United States

*CORRESPONDENCE
Rebecca M. E. Williams,
williams@psi.edu

RECEIVED 18 October 2024
ACCEPTED 28 January 2025
PUBLISHED 21 February 2025

CITATION
Williams RME (2025) Insights from multi-process fan deposits in martian intracrater basins on post-Noachian climate change.
Front. Astron. Space Sci. 12:1513711.
doi: 10.3389/fspas.2025.1513711

Insights from multi-process fan deposits in martian intracrater basins on post-Noachian climate change

Rebecca M. E. Williams*

Planetary Science Institute, Tucson, AZ, United States

Alluvial fans are a sensitive record of environmental transitions. Prior studies have determined that martian fans are primarily located in impact crater basins and that fan deposition occurred principally between 3.7 and 3.3 Ga or later, corresponding to the presumed critical climate-changing period. This paper illustrates previously unrecognized flow types and superposition relationships in fan deposits that show a time sequence of varying processes. Examples include debris flows following earlier eroded fluvial deposits (ridges interpreted as inverted channels), an intriguing pitted deposit interpreted to be a highly viscous mudflow with air bubble release, and landforms recording the role of late-stage fluvio-glacial processes. The diversity of fan forms highlight the complex and variable conditions on post-Noachian Mars. This evidence supports fluctuating 'warm, wet' and 'cold, dry' periods, suggesting that the climate transition was variable and slowly degraded, rather than a swift monotonic decline.

KEYWORDS

alluvial fans, debris flows, inverted channels, Mars morphology, unconformity, surface processes

1 Introduction

The climatic history of Mars remains one of the principal fields of study in the planetary sciences. Constraining the relative timing and duration of aqueous periods based on the geologic record is of fundamental importance to an accurate characterization of past climate conditions on Mars, and by association, determining habitable periods at the planet's surface (Hynek, 2016). Alluvial fans are landforms that can provide insight into this critical question because their flow processes have discriminable differences in the resulting deposits that can be directly tied to water volume and duration. Large alluvial fans in martian highland craters have been interpreted as evidence of a late-stage period of aqueous activity between Early Hesperian and Early Amazonian (3.7–3.3 Ga; e.g., Grant and Wilson, 2011; Mangold et al., 2012; Morgan et al., 2022). The fans preserve the record of Mars' climatic transition from a warmer and wetter early history to the cold and dry Mars we observe today (e.g., Wordsworth, 2016; Ramirez and Craddock, 2018).

On Earth, an active area of research is identifying climatic influences archived in alluvial fan deposits (Bull, 1991; Harvey and Wells, 2003; Lehmkuhl and Owen, 2024). Applying insights from the terrestrial sedimentary record to Mars, this study seeks to glean new details on climate change from the processes involved in fan construction. Was alluvial fan formation associated with a single event, such as wet conditions arising from a volcanic eruption (e.g., Greeley, 1987) or impact event (e.g., Segura et al., 2002)? Or were wet conditions associated with a sustained warmer climate regime that would permit repeated periods of fan formation (e.g., Kite et al., 2017)? Select alluvial fans are illustrated in this work to highlight new details relevant to the question of persistent or repeated surface habitability on Mars.

2 Background

2.1 Terrestrial alluvial fans

An alluvial fan is a semi-conical form that occurs when water-transported material emerges from an upland onto a lowland. Criteria for the development of alluvial fans include 1) topographic setting where an upland is adjacent to a lowland, 2) sufficient sediment supply in the drainage basin and 3) sufficient fluid to transport that sediment out of the drainage basin (Blair and McPherson, 2009). On Earth, arid zone alluvial fans typically build up as successive sheets and lobes of material are transported associated with high magnitude, short duration release of water from rain storms or rapid snowmelt. Morphological characteristics of the terrestrial alluvial fan system include the drainage basin, feeder channel, apex, incised channel, distributary channels, intersection point, and active depositional lobe. The drainage basin is composed of a branching network of tributary channels. The highest order stream, the feeder channel, leads to the most proximal portion of the fan, the apex. In cases where the feeder channel has cut into a pre-existing fan surface to form an incised channel, the intersection point marks the confluence between the channel floor and fan surface. At this point, flows laterally expand and sediment aggradation occurs downslope in an area termed the active depositional lobe. Entrenched or incised channels in fans are due to changing conditions such as increased precipitation, tectonic uplift or a decrease in sediment supply in the headward regions. Terrestrial alluvial fan research has focused on elucidating the roles of climatic, hydrologic, tectonic and lithologic factors controlling fan development (e.g., Beaty, 1990; Bull, 1977; Bull, 1991; Harvey, 1987; Harvey, 1997; Stainstreet and McCarthy, 1993; Lehmkuhl and Owen, 2024).

Terrestrial alluvial fan aggradation can be broadly defined into two end member processes: 1) sediment-gravity processes wherein large volumes of sedimentary material, including interstitial fluid, if any, are transported downslope under the influence of gravity as a direct result of the reduction of ground stability or resisting forces, and 2) fluid-gravity (water-flow) processes that result from precipitation or snowmelt-fed surface runoff that transports sediment downslope (e.g., Blair and McPherson, 2009; Ventra and Clarke, 2018). Fan morphology differentiates between these two end-member depositional processes. Identifying fan aggradation process provides constraints on the amount of fluid and timescale of fan formation. Debris flows, a sediment-gravity process, emplace large volumes of sediment with relatively little fluid component (47%–77% sediment concentration by volume; Costa, 1988) in short periods of time. In contrast, alluvial fans constructed primarily of fluvial processes (sediment concentration in water flows <20% by volume; hyperconcentrated flows 20%–40%; Costa, 1988) build fans incrementally by small amounts typically associated with low occurrence, high magnitude storms. Godt and Coe (2003) identify three types of initiation processes for debris flows: (1) soil slips and (2) overland flow concentrated in steep bedrock-lined channels (i.e., "firehose"), and 3) mobilization of eroded material from steep, non-vegetated hillslopes by a system. Morphostratigraphy of alluvial fans is typically mapped in aerial images, a technique that is used to link geomprohology to formation mechanisms and climate (e.g., Stock, 2013; Ventra and Clarke, 2018; Lehmkuhl and Römer, W., 2022; Lehmkuhl and Owen, 2024). In this study, we draw especially on recognized martian analog sites with arid to hyperarid climates during fan formation (e.g., Harvey, 1997; Morgan et al., 2014; Ritter et al., 2018; Woor et al., 2023).

2.2 Martian alluvial fans

Although it has long been recognized that Mars has undergone dramatic climate change (e.g., Sagan et al., 1973), considerable ambiguity and disagreement remains. The uncertainty surrounding Mars' climate is often framed as a debate between two opposing models: a "warm and wet" climate versus a "cold and wet" climate (Bishop et al., 2018; Fairén, 2010; Head and Marchant, 2014; Wordsworth, 2016). With global temperatures consistently above the freezing point of water, a "warm and wet" climate permits the sustained presence of liquid water (Ramirez and Craddock, 2018). Key evidence supporting this model includes widespread valley networks and lacustrine deposits (Fassett and Head, 2008; Hynek et al., 2010), which suggest long-term surface water activity (Craddock and Howard, 2002). In contrast, the "cold and wet" climate scenario is defined by surface temperatures remaining below freezing for most of Mars' history, with brief intervals of warming triggered by sporadic events such as meteor impacts or volcanic activity (Ramirez and Craddock, 2018; Segura et al., 2002; 2012; Adams et al., 2025). The crux of the paradox is the inconsistency between theoretical and observational evidence (Hynek, 2016): climate models are better able to replicate cold-wet conditions (e.g., Wordsworth et al., 2015; Wordsworth et al., 2016), whereas several studies based on the geologic evidence support warm-wet conditions beyond the Noachian-Hesperian boundary (~3.7 Ga) albeit with poor timing constraints and the possibility of regional rather than global conditions (e.g., Davis et al., 2016; Davis et al., 2019; Kite et al., 2017; Morgan et al., 2022; Kite and Conway, 2024; Holo et al., 2021). Recently, Adams et al. (2025) performed modeling that demonstrated that episodic warm, wet conditions could occur into the Hesperian due to H_2 release from water-rock interactions supplemented by transient volcanic activity.

There is widespread recognition that a better handle on the timing and duration of surface aqueous conditions post-Noachian is needed to meaningfully advance understanding of the martian climate evolution (e.g., Kereszturi, 2012; Changela et al., 2021). On Mars there are few opportunities to interrogate the climate conditions during the post-Noachian epoch, due to the paucity of the martian geologic deposits available to assess via orbital remote sensing data. Understanding the paleo-hydrologic conditions and timescales of aqueous activity based on the formation of alluvial fans at sites around the globe contributes to a better understanding of the history of water on Mars and is a critical component to identifying past climate conditions and habitable regions.

Despite evidence of fluvial erosion in the form of valleys and outflow channels, sedimentary deposits associated with such landforms are relatively rare on Mars. The existence of depositional basins was hypothesized from Viking images (e.g., Goldspiel and Squyres, 1991), and several studies noted degradation of landforms such as craters (e.g., Craddock and Howard, 2002). Many of the proposed sites for fan deposits based on knobs and mesas located near the termini of valleys that breach crater walls in Viking images (Cabrol and Grin, 1999; 2001) do not show evidence of deposition in the higher resolution data (e.g., note 22 in Malin and Edgett, 2003; Irwin et al., 2005). However multiple examples of fan-shaped depositional landforms were recognized in martian crater basins with higher resolution images and elevation data in the post-Mars Global Surveyor (MGS) era (e.g., Malin and Edgett, 2003; Moore et al., 2003; Moore and Howard, 2005; Irwin et al., 2005 and references therein; Fassett and Head, 2005; Williams and Malin, 2008; Di Achille and Hynek, 2010a; Di Achille and Hynek, 2010b).

Recently, Wilson et al. (2021) published an inventory of martian fans that built on earlier catalogs (e.g., Moore and Howard, 2005; Kraal et al., 2008). Wilson et al. (2021) conducted a comprehensive, global survey of Mars using high resolution image data (ConTeXt Camera, CTX; 6 m/pix) to map fan-shaped deposits within impact craters. They subdivided these landforms into categories based on their morphological attributes and interpreted origin. Ultimately, they identified 890 alluvial fans located within 206 craters (Figure 1). In their study, alluvial fans were differentiated from fans with ambiguous origin, and scarp-fronted fans that are inferred to be deltaic deposits (e.g., Di Achille et al., 2006; Di Achille et al., 2010a; Di Achille et al., 2010b; Goudge et al., 2017), although post-deposition erosion of an alluvial fan is acknowledged as an alternative explanation. Whilst most (70%) alluvial fans apparently formed contemporaneously with valley network activity, a considerable fraction (30%) of alluvial fans formed well after the era of valley networks spanning from Early Hesperian to Middle Amazonian (Morgan et al., 2022).

3 Materials and methods

3.1 Data

Data for this project is publicly released and archived at the Planetary Data System (PDS) Geoscience Node. Data was co-registered using ESRI ArcGIS software, as well as JMARS (Java Mission-planning and Analysis for Remote Sensing) (Christensen et al., 2009). Image datasets examined are the Mars Odyssey Thermal Emission Imaging System (THEMIS, Christensen et al., 2009) images from the infrared (IR, 100 m/pix) and visible (VIS, 18 m/pix) cameras, Mars Express High Resolution Stereo Imager (HRSC, up to 2.3 m/pix; Jaumann et al., 2007), Mars Reconnaissance Orbiter (MRO) Context Imager (CTX, 6 m/pix; Malin et al., 2007; global mosaic by Dickson et al. (2024), MRO High Resolution Imaging Science Experiment (HiRISE, up to 25 cm/pix; McEwen et al., 2007), and Mars Orbiter Camera (MOC, 1.5–12 m/pix; Malin and Edgett, 2003) images.

Topographic analysis used several datasets, including from the Mars Global Surveyor Mars Orbiter Laser Altimeter (MOLA, Zuber et al., 1992) supplemented with high-resolution stereo-derived topography from HRSC (50–75 m/pixel). The HRSC DEM (Jaumann et al., 2007) is produced by the HRSC team and available from the *HRSCView* website. Higher resolution DEMs were generated using the NASA Ames Stereo Pipeline (Beyer et al., 2018) for CTX following work by Shean et al. (2011). Resulting products with CTX (~10 m/pixel; ~10 m vertical precision) are archived at DEMs https://Doi.org/10.5066/P9I1QO1U. Where available and publicly released, we also examined HiRISE (~1 m/pix. ~0.2 m vertical precision).

THEMIS-derived quantitative thermal inertia from the global mosaics is used to characterize material properties of fan surfaces (Fergason et al., 2006; Christensen and fergason, 2013). Material properties of the surface are reflected in the thermal inertia, which is sensitive to particle size, porosity and compaction (e.g., Fergason et al., 2006; Edwards et al., 2009). Thermal inertia (TI) is defined as $(k\rho c)^{1/2}$, where k is the bulk thermal conductivity, ρ is the bulk density, and c is the specific heat of the material (Kieffer et al., 1977). Higher thermal inertia values are associated with mechanically strong substrates, such as well-indurated rocks. Lower thermal inertia values correspond to mechanically weak surfaces, such as friable or weakly consolidated rocks and/or dominantly fine-to-medium sand-sized clasts.

3.2 Approach

Martian alluvial fans are an inherently closed sedimentological and hydrological system (source to sink). As depositional features in close proximity with a sediment source, alluvial fans preserve a record of the prevailing climate during the transport and deposition of sediment within their stratigraphy. There is a well-established history of utilizing alluvial fans to decipher past climatic conditions on Earth (e.g., Havrey and Wells, 1994; Havrey and Wells, 2003; Harvey, 2003; Haug et al., 2010; Salcher et al., 2010). In this study, the martian alluvial fan morphology is characterized through mapping, based on terrestrial analogs.

This study seeks to reconstruct the aqueous history on Mars through detailed morphological analysis of understudied alluvial fans, which may have been former habitable environments. Following a visual inspection of high resolution images for all intracrater alluvial fans in Wilson et al. (2021), twenty-seven sites (13%) were identified for further detailed study (Figure 1; Supplementary Table S1). Selected sites had noteworthy attributes pertinent to the study objectives with possibly insightful aspects related to flow process and/or stratigraphic context. High resolution images and digital elevation models (DEMs) from the CTX and HiRISE instruments were used to differentiate sediment-gravity flow deposits from fluid-gravity deposits, as well as the superposition relationships between deposits, to develop an evolutionary sequence.

Maximum age for the alluvial fans is based on the crater-dated geologic unit that underlies the fan-hosting crater in the Tanaka et al. (2014) global geologic map of Mars, as reported in Wilson et al. (2021) (Supplementary Table S1). Six age groups are as follows: 1) Amazonian-to Hesperian-age impact craters

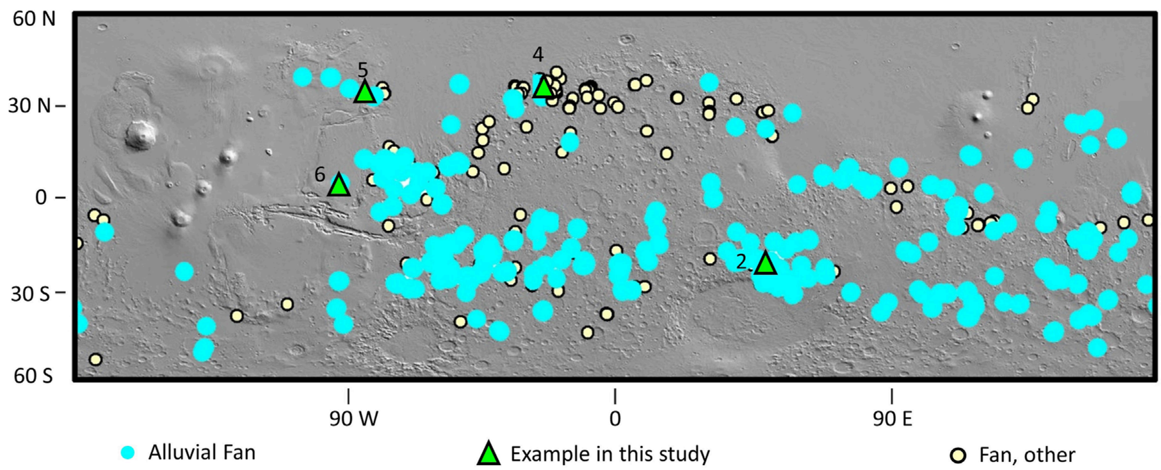

FIGURE 1
Locations of martian fans and their classification (alluvial fan or other) from Wilson et al. (2021) are shown superimposed on MOLA shaded relief map, with alluvial fans. Fans inferred as deltaic (scarp-fronted) or equivocal in origin are grouped here as "Fan, other" marked by yellow circles, and constitute a modest component of the martian fan inventory (15%). Alluvial fan examples illustrated in this study are marked by green triangle and labeled by figure number.

(impact unit), 2) Hesperian (includes Early and Late Hesperian), 3) Hesperian to Noachian (transition unit), and 4) Noachian (includes Early, Middle, and Late Noachian). In some cases, additional information is available that refines the alluvial fan age, such as crater counts on the fan surface (Supplementary Table S2). Although the presence of embedded craters in alluvial fan stratigraphy has been observed (Kite et al., 2017), none of the selected sites have reported embedded craters.

4 Results

4.1 Composite alluvial fans (superposition relationships)

One of the greatest concentrations of alluvial fans on Mars is in southwestern Tyrrhenna Terra (Moore and Howard, 2003). Anderson et al. (2022) reported on variations in fan morphology in five intracrater basins. These findings are expanded here to discuss details of fan building process by illustrating deposit morphology and superposition relationships. Finally, an example from the northern hemisphere is presented with similar attributes, and a noteworthy difference.

Figure 2 illustrates the sharp transition from a chute-dominated upper fan, to ridges and lobes downslope. On the upper fan, linear chutes are ~250 m wide and radiate from the fan apex, reflecting shifting flow paths. Deposits at the termination of chutes have a lobate form, strongly suggesting debris flow processes. Subjacent to these lobes are radiating ridges. Ridges are 50–100 m wide and exhibit subtle relief of up to a few meters. The ridges exhibit low sinuosity and branch downslope consistent with the planimetric pattern of distributary channels. The ridges are interpreted as the erosional remnants of fluvial flows (e.g., inverted channels). The clear superposition between upper lobes and distal ridges is shown in Figure 3, marking an unconformity. This fan deposit pattern is observed in several (~40%) alluvial fans regionally (Anderson et al., 2022), and observed in the global survey of this study although not tabulated. In a second example, Figure 2E shows the fan feeder channel transitions to a chute with three stacked lobe deposits.

For fans with composite deposits there is often a sharp thermal boundary between the upper and lower fan (Figures 2B, D). In Figures 2C, D; Supplementary Figure S1, the thermal inertia values for the ridged portion of the fan is elevated relative to the upper fan with lobes (difference of ~50 $Jm^{-2}K^{-1}$ $s^{-1/2}$). This trend is interpreted to reflect a combination of lithified material and erosional removal of fine grain particles.

Many alluvial fans on Mars have ridges in their distal portions. Figure 4 illustrates an example in northern Arabia Terra. The terraced fan deposit superposes thin ridges radiating downslope (Figure 4B). In contrast to the fans in Tyrrhenna Terra, there are stacked ridges on the crater floor that record multiple fluvial events (Figure 4C). However, the association of these crater floor ridges to the alluvial fans is unclear, as they are spatially separated landforms.

4.2 Pitted textures on alluvial fan deposits

Through the systematic review of the larger alluvial fan sites, a few exemplary locations demonstrate a surprising link between surface texture and flow process. In a Tempe Terra crater, Figure 5 shows the continuity relationships of the deposit from alcove mouth to the crater floor where the pitted deposit terminates in an escarpment. The deposit drapes over a topographic bench, an indication of the material properties of the flow. High viscosity and material strength are required for the flow to coat the escarpment. A sedimentary origin is preferred due to the origin of the flow from a crater rim alcove, and the lack of volcanic source. Some pits on the fan surface are likely impact craters, such as the double pit in Figure 5B. However, the spatial distribution of the

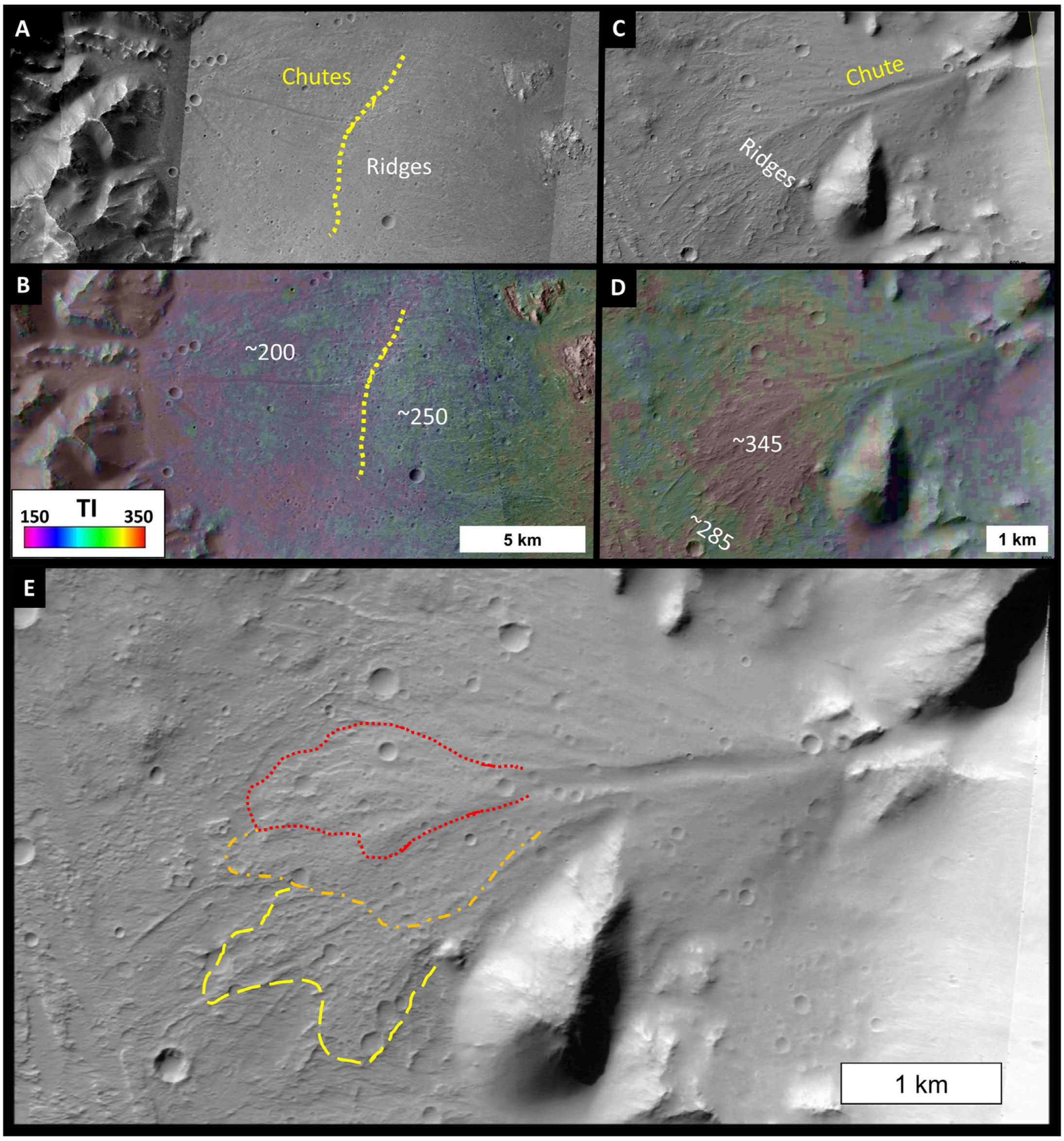

FIGURE 2
Illustration of alluvial fans within crater located near 22.45^0 S, 76.71^0 E. **(A, C)** Alluvial fans on the west and east sides of the crater, respectively, have chute and ridge morphology. **(B, D)** THEMIS-derived quantitative thermal inertia from the global mosaic (Christensen and Fergason, 2013) shows thermal properties differ between fan morphology types. Ridges exhibit higher thermal inertia values relative to terrain with chutes. TI = thermal inertia units, $Jm^{-2}K^{-1}s^{-1/2}$. See also Supplementary Figure S1. **(E)** Enlargement of panel C to illustrate distal ridges (inverted channels) and proximal multiple, superposing lobes in alluvial fan on the eastern side of crater near 22.45^0 S, 76.71^0 E. Subscenes of CTX image J02_045480_1574_XI_22S283W with illumination from lower left. Figures generated using the JMARS tool (Christensen et al., 2009) with CTX global mosaic basemap (Dickson et al., 2024).

circular pits is problematic for an impact crater interpretation for the pitted texture of the fan. The high density and size configuration (concentrated in areas where the flow bends around obstacles) is atypical for a cratered terrain. The observational evidence supports the interpretation of a mudflow origin for pitted terrain texture.

In Xanthe Terra, a pitted texture is present on a thin fan deposit (Figure 6). The flow extends nearly 30 km from the two source alcoves on the crater rim. The flow appears to be a contiguous deposit, with no identifiable lobes or superposition relationships. This suggests that a single triggering event mobilized sediment from both alcoves simultaneously. The pitted texture is associated with the distal portions of the deposit. The crenulated margin (Figure 6B) indicates high material strength of the flow deposit.

5 Discussion

5.1 Time-varying flow processes

Variations in alluvial fan morphology may represent different periods of fan formation. In some cases, alluvial fans transition from chutes and lobes to ridges (channels in inverted relief)

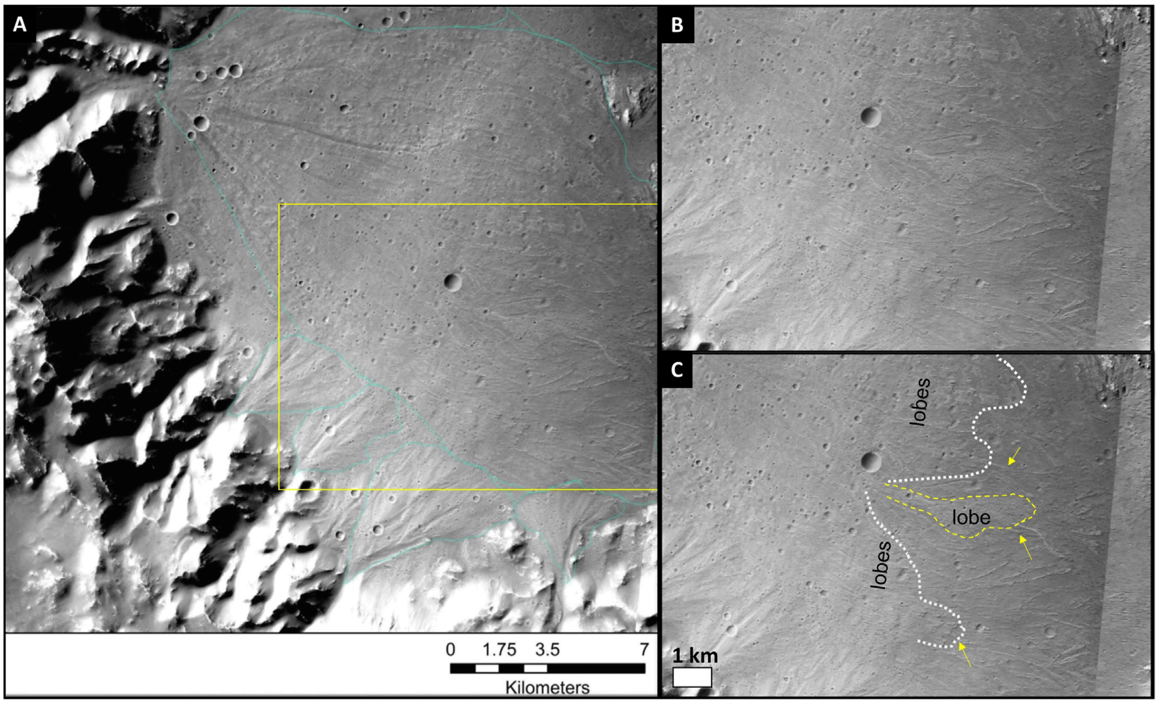

FIGURE 3
(A) Alluvial fans (pale green outlines) on the western side of crater near 22.45° S, 76.71° E (Figure 2A). The largest fan has a cratered surface. **(B)** is enlargement to illustrate the fan textures, annotated in panel **(C)** of various lobe margins and distal ridges (yellow arrows). Subscenes of CTX image D16_033559_1585_XI_21S283W with illumination from lower left.

at their distal ends (e.g., Figure 2; Anderson et al., 2022). This trend was previously interpreted as preferential erosion exploiting downfan fining of deposits and leaving the upper fan protected by coarser deposits (e.g., a single-phase of fan deposition, Figure 7A; DiBiase et al., 2013). Alternatively, composite fan morphology could result from burial of an older, denuded fan surface (inverted channels across entire fan) by a later stage of alluvial fan activity (chutes and lobes). This sequential fan formation is the multi-phase model (Figure 7B), the favored interpretation in this work. The superposition relationships reported here (Section 4.1), signifies an unconformity (depositional hiatus associated with deflation) that reflects a time sequence change in depositional process: fluvial flows to debris flow.

Additional evidence in support of the multi-phase model is the distinct thermal boundary between fan morphology types (Figure 2; Supplementary Figure S1). The observed sharp thermal contact correlated to fan morphologic types is consistent with material property variations associated with fluvial and debris-flow deposits. In contrast, the single-phase model should produce a more subtle thermal signature. Although a purely fluvially-formed alluvial fan would be expected to have a decreasing thermal inertia signature downfan due to the downslope fining of clasts, the particle size effects would be less pronounced under the single-phase formation hypothesis due to removal of sand-size particles during deflation. With differential erosion removing distal fines, the thermal inertia signature across the fan surface would be uniform or gradational downfan, reflecting the transition from coarser material armoring the proximal fan and indurated materials (corresponding to inverted channels) on the distal fan. (However, it must be acknowledged that interpretation of thermal inertia data is non-unique. Furthermore, Mondro et al. (2024) demonstrate that almost all martian fans (99%) exhibit no discernible spatial pattern in surface thermal inertia, and the homogenous values are consistent with a fines-dominated surface due to sand from depositional, widespread mantling and/or *in situ* weathering.)

The commonality of this specific type of alluvial fan superposition relationship (composite alluvial fan) in multiple crater basins may reflect changes in water availability. The pervasiveness (but not ubiquitousness) of this unconformity across the globe suggests that climate conditions may be responsible. Fluvial flows may be generated via precipitation patterns. Lesser water volumes are needed for debris flows, which could be seasonally triggered by meltwater. Importantly, both flow processes require clement climate conditions for surface water flow.

5.2 Mudflows

Commonly circular depressions on Mars are interpreted almost exclusively as impact craters. However, puzzling superposition relationships have been noted in areas where the older buried terrain exhibits a significantly lower crater density than the younger, topmost strata (Malin and Edgett, 2000; for an illustration see Figure 3 in Edgett and Sarkar, 2021). One explanation for this

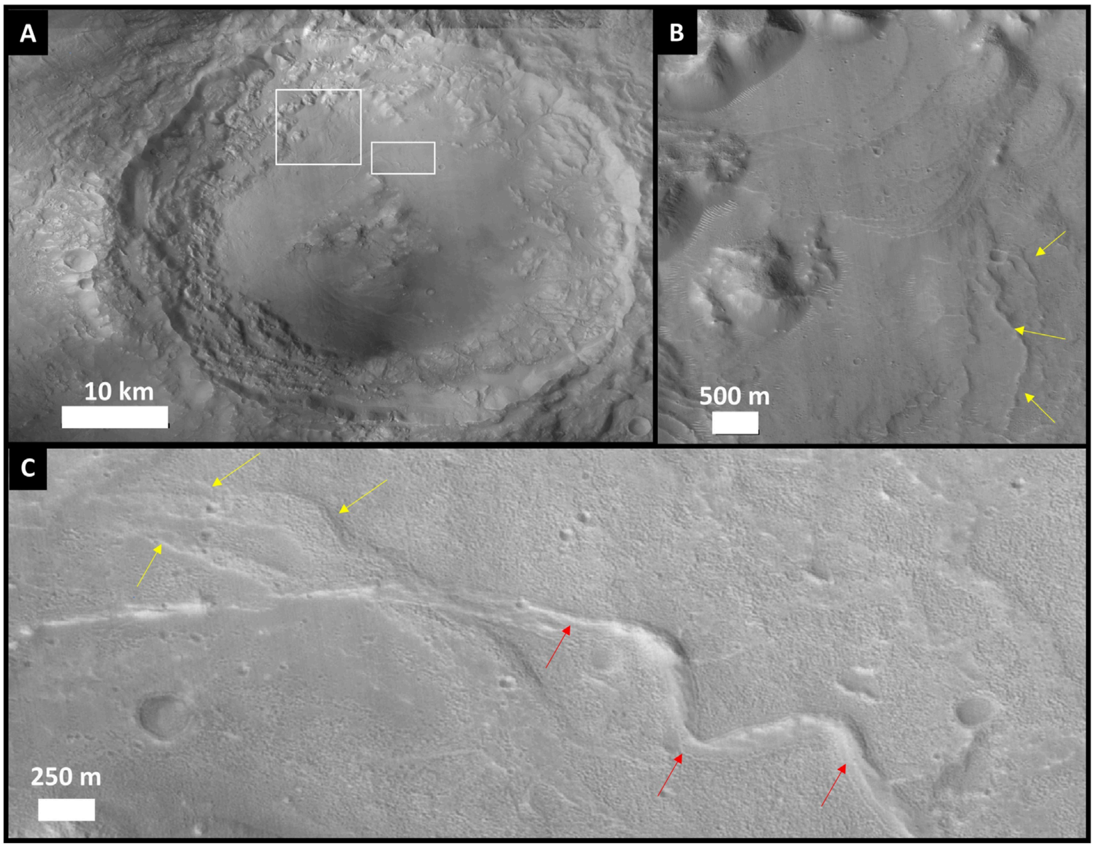

FIGURE 4
(A) Alluvial fans within an unnamed crater near35.6^0 N, 0.6^0 E are mostly small deposits. **(B)** In the northern portion of the crater is a large, terraced alluvial fan. Beyond the distal margin of the fan deposit there are ridges (yellow arrows). **(C)** On the crater floor, two generations of ridges are present, with older, wide bands (yellow arrows), superposed by sinuous thin ridges (red arrows). Figure generated using the JMARS tool (Christensen et al., 2009) with CTX global mosaic (Dickson et al., 2024).

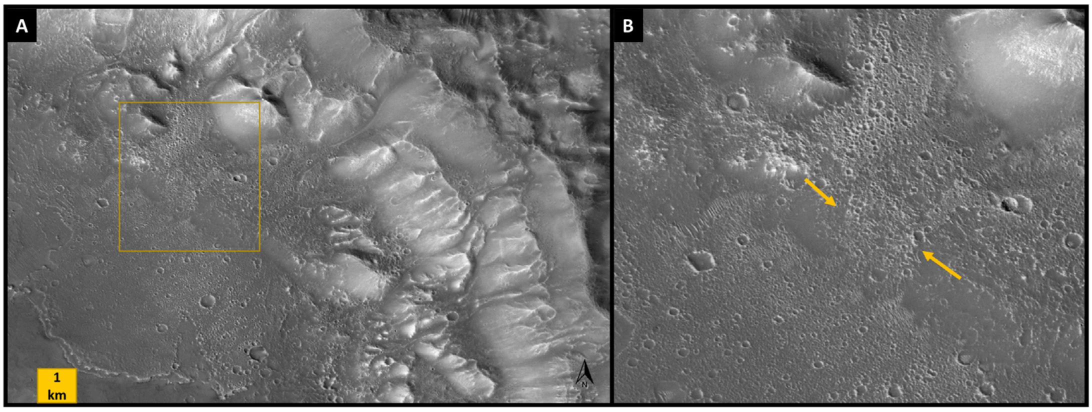

FIGURE 5
(A) Morphological evidence of mudflow in crater near 32.6^0 N, 301.8^0 E. Left panel shows the fan-shaped feature that originates from linear alcove on crater rim and terminates in arcuate escarpment at lower left. **(B)** Enlargement (orange box) shows continuity of pitted terrain draped across topographic escarpment (topographic brink point marked by arrows). Subscenes of CTX ImageJ14_050337_2129_XN_32N058W with illumination from lower left.

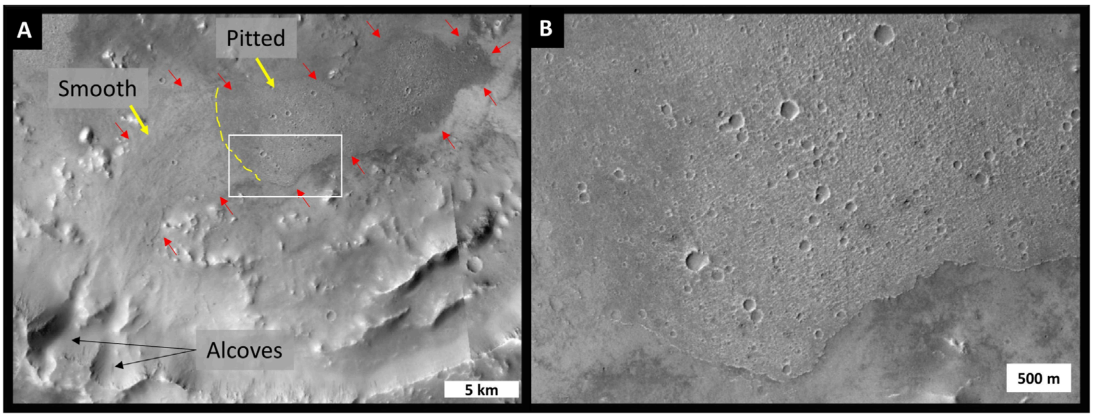

FIGURE 6
(A) Martian fan within crater was sourced from dual alcoves. The deposit, outlined by red arrows, has a textural change downslope from a relatively smooth surface to one with a high density of pits. **(B)** Enlargement of pitted texture with crenulated margin (bottom of image). Location is near 4.5^0 N, 69.2^0 W. Subscenes of CTX image G22_026681_1841_XN_04N069W with illumination from lower left.

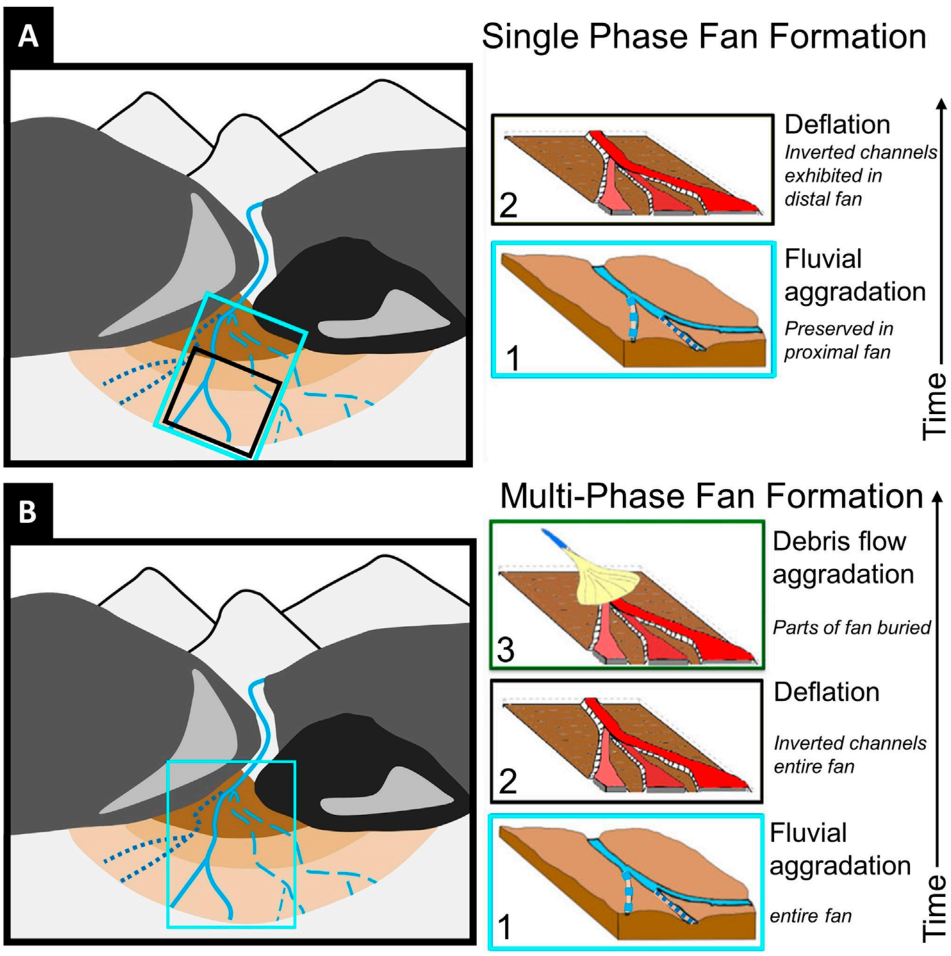

FIGURE 7
Schematic illustrating two hypotheses to explain composite alluvial fan morphology: differential erosion (single-phase hypothesis in **(A)**) and sequential fan formation (multi-phase hypothesis in **(B)**). Both cases begin with fluvial aggradation, represented schematically with blue distributary channels (solid line for active channels and dashed and dotted lines for two generations of abandoned channels from successive avulsions). Figure is adapted from DiBiase et al., 2013.

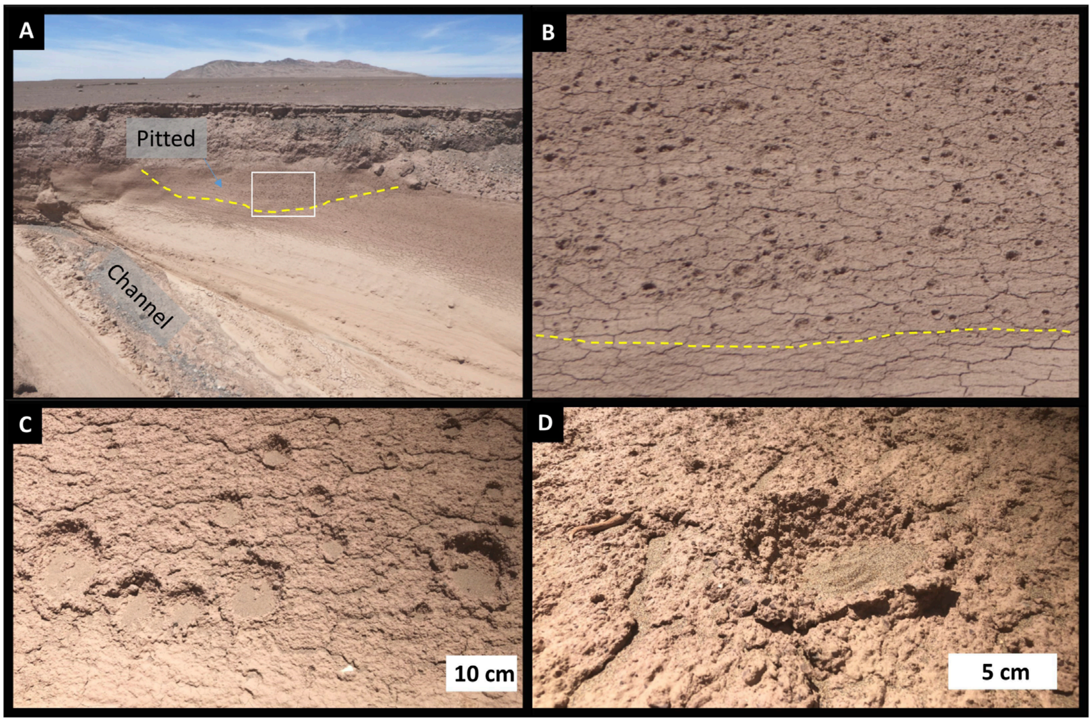

FIGURE 8
(A) Localized pitted texture is present on margin of mudflow along canyon wall in Quebrada de Guatacondo, Chile. Yellow dashed line marks the boundary of pitted texture. Site is near −21.01783 S, −69.36036 W. **(B)** Hemispherical cavities are tens of centimeters across. **(C)** Image orthogonal to surface shows the spatial distribution of cavities. **(D)** Close-up of elliptical pit with raised rim (shadow at lower right).

paradox is different material properties of the terrain, such that the impact crater record is not preserved (e.g., erased by erosion). In this paper, examples of fan deposits with pitted terrain (Figures 5, 6) are evidence that flow processes can be involved in the generation of circular depressions, and this alternative explanation could be considered in evaluating cratered landscapes.

Subsurface volatile release is a mechanism to generate pitted terrain. Migration of buoyant materials through unconsolidated, fluid-saturated layers produces soft-sediment deformation structures. For example, gas bubble migrations through mud deposits at Lake Powell, Utah form cavities tens of meters in diameter (Sherrod et al., 2016; Miller et al., 2018), and larger structures (hundreds of meters) are documented in marine settings (e.g., Cole et al., 2000; Barry et al., 2012). In modern fluvial and pond settings, pressurized water exits vertically through sand and/or clay deposits to create decimeter-scale pits or pockmarks (e.g., Holzer and Clark, 1993; Guhman and Pederson, 1992; Draganits and Janda, 2003).

These examples are noteworthy in the configuration of the cavities with space between pits or pit clusters, a spatial distribution that differs from periglacial space-filling pitted terrain. On Mars, sublimation ice loss driven pitted pattern (e.g., Ramsdale et al., 2018) are larger scale surface textures that typically blanket the landscape and are distinct from the pits shown here that are confined to the fan surface (Figures 5, 6).

A related mechanism to soft-sediment hemispherical cavities described above is air escape from a sedimentary flow that could generate pitted terrain. Apparently not previously documented, this paper presents a terrestrial analog for the martian pitted textures on a mudflow deposit in the Atacama Desert of northern Chile. Although the Chilean pits are much smaller in scale, they have many morphological and distribution attributes in common with the martian pits illustrated in Figures 5, 6.

Along the banks of the Quebrada de Guatacondo, centimeter-scale circular-to-elliptical pits are present in a mudflow deposit on the canyon walls but absent in the channel (bypass flow; Figure 8). In the Quebrada de Guatacondo mudflow deposit, hemispherical cavities decrease in size upslope (Figure 8B). Measurements of a representative maximum pit show the size change: near the channel margin (18 × 16 × 6 cm) to high on the slope (6.5 × 5 × 2 cm). The largest pits are where flow is thickest, near break in slope by the channel. Cavities are cross-cut by polygonal cracks indicating they formed prior to desiccation of the deposit (Figure 8B). Some pits have raised rims (Figure 8D).

The mudflow was viscous and turbulent, resulting in a deposit that is draped on the steep canyon walls (superelevation). Morgan et al. (2014) estimated 1–2 m flow thickness based on run-up distance. The vigorous flow trapped air that escaped prior to the flow drying out. If the mechanism is the same for martian pitted terrain (e.g., highly viscous mudflow with air bubble release), it places constraints on the climate conditions present during the flow.

5.3 Ice-based processes associated with alluvial fans

Recently, several authors have interpreted ridges on crater floors as due to glacio-fluvial processes (e.g., Zhang et al., 2023; Grau Galofre et al., 2024). One concentration is on nineteen crater floors in southeastern Terra Sabea (Gullikson et al., 2023) where dominantly radial ridges and a few circumferential ridges are associated with proglacial paleolakes (Boatwright and Head, 2021; Boatwright and Head, 2022). In the northern hemisphere, a few examples of radial ridges linked to ice-related landforms such as viscous flow features or moraines (Gallagher and Balme, 2015; Butcher et al., 2017; Butcher et al., 2021). The present study expands the locations where this landform type is recognized. Figure 4 illustrates potential examples of glacio-fluvial landforms (Williams et al., 2024). The circumferential ridges in Figure 4C (yellow arrows) are visually similar to the flat-crested ridges in Terra Sabea (e.g., see Figure 18 in Boatwright and Head, 2022). In addition, Boatwright and Head (2022) suggested that ridge stacking in Terra Sabea could be inverted proglacial fluvial channels associated with episodic generation of glacial meltwater, a possible explanation for the configuration in Figure 4C.

Wilson et al. (2016) acknowledged the ambiguity in interpreting the fan-emanating radial ridges in Figure 4B as either candidate eskers or inverted channel (e.g., Figure 7). Distinguishing an esker origin from inverted channel is challenging (Boatwright and Head, 2022), especially as both landforms could co-exist as illustrated in Chukhung crater by Butcher et al. (2021). Although an exclusively inverted channel origin for the ridges shown in Figure 4 is a plausible alternative interpretation, a lava-capped inverted channel is specifically disfavored due to lack of supporting contextual evidence and the relative uncommon occurrence of such features. Volcanic rock-capped inverted channels are relatively rare on Earth constituting <25% of the inverted channel catalog, and these examples do not exhibit stacked ridges as shown in Figure 4C (Zaki et al., 2021). Likewise, few martian inverted channels are inferred to be lava capped. One example is Mangala Valles (Keske et al., 2015) and is distinguished from the features in Figure 4 in several important ways: a direct link to a volcanic source region, surface textures consistent with lava flows and the significantly larger scale of the landform (valley filling).

The proposition of combined glacier and fluvial landforms in the ridges of this northern Arabia Terra crater is bolstered by regional evidence for glaciation. There are ice-rich deposits in nearby Deuteronilus Mensae (Berman et al., 2015) with morphologies that extend to this crater (Williams et al., 2024). Also, the recognition of mid-latitude fresh shallow valleys, including ones adjacent in the so-called "Heart Lake" system, formed from snowmelt-based hydrology that occurred during the Hesperian-Amazonian transition (Wilson et al., 2016). Consistent with that timing, Berman and Williams (2025) report crater counts on the ejecta blanket yield a crater formation age of ~3.4 Gyr in the middle Hesperian, but note considerably younger crater retention ages for the fan deposits due to modification, ~110 and 370 Ma in the early Amazonian. Further study of this complex site is needed to understand the association of alluvial fans and the ridges in terms of relative timing of fan aggradation and potential glaciation.

6 Conclusion

Martian alluvial fans deposition largely coincided with a key climate transition period. From a survey of large alluvial fans, this paper documents a variety of fan forms and superposition relationships that underscore the complex and fluctuating conditions on post-Noachian Mars. This evidence indicates a gradual and variable climate decline rather than a rapid, uniform change.

1) Multiple crater basins have alluvial fans with a characteristic unconformable deposit: upper fan lobes emplaced by debris flows superposing distal fan ridges, the erosional remnants of fluvial processes.
2) Documented for the first time here, fan deposits with pitted textures. Drawing parallels to a terrestrial analog, the pitted texture likely formed by a highly viscous mudflow releasing air bubbles.
3) Radial and circumferential ridges on the floors of some craters hosting alluvial fans warrant further study. These ridges add to a growing list of sites interpreted as candidate glacio-fluvial landforms. The relative timing of fluvio-glacial processes compared to the fan forming events is unclear.

Data availability statement

The datasets presented in this study can be found in online repositories. The names of the repository/repositories and accession number(s) can be found below: https://doi.org/10.5066/P9I1QO1U and at NASA's Planetary Data System (PDS) Geoscience Node https://pds-geosciences.wustl.edu/.

Author contributions

RW: Conceptualization, Data curation, Formal Analysis, Funding acquisition, Investigation, Methodology, Project administration, Resources, Validation, Visualization, Writing–original draft, Writing–review and editing.

Funding

The author(s) declare that financial support was received for the research, authorship, and/or publication of this article. Funding for this research was from NASA Mars Data Analysis Program grant #80NSSC19K1216 and #80NSSC20K0944, and funds to support the Mars Odyssey-THEMIS Extended Mission program (NASW-00002).

Acknowledgments

The author is grateful for conversations on this topic with A. Howard, S. Wilson Purdy, A. Morgan, D. Berman, B. Hynek, M. Malin, R. Anderson and A. Gulikson. She appreciates the constructive feedback from J. W. Head and an reviewer. This research

used the JMARS (Java Mission-planning and Analysis for Remote Sensing) geospatial information system tool developed by ASUs Mars Space Flight Facility (Christensen et al., 2009).

Conflict of interest

The authors declare that the research was conducted in the absence of any commercial or financial relationships that could be construed as a potential conflict of interest.

Generative AI statement

The author(s) declare that no Generative AI was used in the creation of this manuscript.

Publisher's note

All claims expressed in this article are solely those of the authors and do not necessarily represent those of their affiliated organizations, or those of the publisher, the editors and the reviewers. Any product that may be evaluated in this article, or claim that may be made by its manufacturer, is not guaranteed or endorsed by the publisher.

Supplementary material

The Supplementary Material for this article can be found online at: https://www.frontiersin.org/articles/10.3389/fspas.2025.1513711/full#supplementary-material

References

Adams, D., Scheucher, M., Hu, R., Ehlmann, B. L., Thomas, T. B., Wordsworth, R., et al. (2025). Episodic warm climates on early Mars primed by crustal hydration. *Nat. Geosci.* doi:10.1038/s41561-024-01626-8

Anderson, R. B., Williams, R. M. E., Gulikson, A. G., and Nelson, W. (2022). Inverted relief and morphology of intracrater alluvial fans north of hellas basin. *Icarus* 394 (115122), 22. doi:10.1016/j.icarus.2022.115122

Barry, M. A., Boudreau, B. P., and Johnson, B. D. (2012). Gas domes in soft cohesive sediments. *Geology* 40, 379–382. doi:10.1130/G32686.1

Beaty, C. B. (1990). "Anatomy of a White Mountain debris flow—the making of an alluvial fan," in *Alluvial fans–A field approach*. Editors A. H. Rachocki, and M. Church (New York: Wiley), 69–89.

Berman, D. C., Crown, D. A., and Joseph, E. C. S. (2015). Formation and mantling ages of lobate debris aprons on Mars: insights from categorized crater counts. *Planet. Space Sci.* 111, 83–99. doi:10.1016/j.pss.2015.03.013

Berman, D. C., and Williams, R. M. E. (2025). *Sub-glacial melting in northern Arabia Terra? Evidence for valley glaciers, meltwater channels, and proglacial lakes*, LVI. Houston, TX: Lunar and Planetary Institute. Available at: https://www.hou.usra.edu/meetings/lpsc2025/pdf/1530.pdf.

Beyer, R. A., Alexandrov, O., and McMichael, S. (2018). The Ames Stereo Pipeline: NASA's open source software for deriving and processing terrain data. *Earth and Planetary Science* 5 (9). doi:10.1029/2018EA000409

Bishop, J. L., Fairén, A. G., Michalski, J. R., Gago-Duport, L., Baker, L. L., Velbel, M. A., et al. (2018). Surface clay formation during short-term warmer and wetter conditions on a largely cold ancient Mars. *Nat. Astron.* 23 (2), 206–213. doi:10.1038/s41550-017-0377-9

Blair, T. C., and McPherson, J. G. (2009). "Processes and forms of alluvial fans," in *Geomorphology of Desert environments*. Editors A. J. Parsons, and A. D. Abrahams (Netherlands, Dordrecht: Springer), 413–467. doi:10.1007/978-1-4020-5719-9_14

Boatwright, B. D., and Head, J. (2022). Inverted fluvial channels in Terra sabaea, Mars: geomorphic evidence for proglacial paleolakes and widespread highlands glaciation in the late noachian–early hesperian planetary and space. *Science* 3 (38), 17. doi:10.1016/j.pss.2022.105621

Boatwright, B. D., and Head, J. W. (2021). A noachian proglacial paleolake on Mars: fluvial activity and lake formation within a closed-source drainage basin crater and implications for early Mars climate. *Planet. Sci. J.* 2, 52. doi:10.3847/PSJ/abe773

Bull, W. B. (1977). The alluvial-fan environment. *Prog. Phys. Geogr. Earth Environ.* 1 (2), 222–270. doi:10.1177/030913337700100202

Bull, W. B. (1991). *Geomorphic responses to climatic change*. New York: Oxford University Press, 326.

Butcher, F. E., Balme, M. R., Conway, S. J., Gallagher, C., Arnold, N. S., Storrar, R. D., et al. (2021). Sinuous ridges in Chukhung crater, Tempe Terra, Mars: implications for fluvial, glacial, and glaciofluvial activity. *Icarus* 357, 114131. doi:10.1016/j.icarus.2020.114131

Butcher, F. E. G., Balme, M. R., Gallagher, C., Arnold, N. S., Conway, S. J., Hagermann, A., et al. (2017). Recent basal melting of a mid-latitude glacier on Mars. *J. Geophys. Res. Planets* 122, 2445–2468. doi:10.1002/2017JE005434

Cabrol, N., and Grin, E. A. (1999). Distribution, classification and ages of Martian impact crater lakes. *Icarus* 142, 160–172. doi:10.1006/icar.1999.6191

Cabrol, N., and Grin, E. A. (2001). The evolution of lacustrine environments on Mars: is Mars only hydrologically dormant? *Icarus* 149, 291–328. doi:10.1006/icar.2000.6530

Changela, H. G., Chatzitheodoridis, E., Antunes, A., Beaty, D., Bouw, K., Bridges, J. C., et al. (2021). Mars: new insights and unresolved questions. *Int. J. Astrobiol.* 20 (6), 394–426. doi:10.1017/S1473550421000276

Christensen, P. R., Engle, E., Anwar, S., Dickenshied, S., Noss, D., Gorelick, N., et al. (2009). JMARS – a planetary gis. Available at: http://adsabs.harvard.edu/abs/2009AGUFMIN22A.06C.

Christensen, P. R., and Fergason, R. L. (2013). THEMIS-derived thermal inertia mosaic of Mars: product description and science results. *Lunar Planet. Sci. Conf.*

Cole, D., Stewart, S., and Cartwright, J. (2000). Giant irregular pockmark craters in the palaeogene of the outer moray firth basin, UK north sea. *Mar. Pet. Geol.* 17, 563–577. doi:10.1016/S0264-8172(00)00013-1

Costa, J. E. (1988). "Rheologic, geomorphic, and sedimentologic differentiation of water floods, hyperconcentrated flows and debris flows," in *Flood geomorphology: New York*. Editors V. R. Baker, R. C. Kochel, and P. C. Patton (Wiley), 113–122.

Craddock, R. A., and Howard, A. D. (2002). The case for rainfall on a warm, wet early Mars. *J. Geophys. Res.* 107 (E11). doi:10.1029/2001JE001505

Davis, J. M., Balme, M. R., Grindrod, P. M., Williams, R. M. E., and Gupta, S. (2016). Extensive Noachian fluvial systems in Arabia Terra: implications for early martian climate. *Geology* 44 (10). doi:10.1130/G38247.1

Davis, J. M., Gupta, S., Balme, M. R., Grindrod, P. M., Fawdon, P., Gupta, S., et al. (2019). A Diverse Array of Fluvial Depositional Systems in Arabia Terra: Evidence for mid-Noachian to Early Hesperian Rivers on Mars. *J. Geophys. Res.* 124. doi:10.1029/2019JE005976

Di Achille, G., and Hynek, B. M. (2010a). Ancient ocean on Mars supported by global distribution of deltas and valleys. *Nat. Geosci.* 3, 459–463. doi:10.1038/NGEO891

Di Achille, G., and Hynek, B. M. (2010b). "Chapter 8: deltas and valley networks on Mars: implications for a global hydrosphere," in *Lakes on Mars*. Editors N. A. Cabrol, and E. A. Grin (Amsterdam: Elsevier), 223–248.

Di Achille, G., Marinangeli, L., Ori, G. G., Hauber, E., Gwinner, K., Reiss, D., et al. (2006). Geological evolution of the tyras vallis paleolacustrine system, Mars. *J. Geophys. Res.* 111 (E4), 19. doi:10.1029/2005JE002561

DiBiase, R. A., Limaye, A. B., Scheingross, J. S., Fischer, W. W., and Lamb, M. P. (2013). Deltaic deposits at Aeolis Dorsa: sedimentary evidence for a large body of water in the northern plains of Mars. *J. Geophys. Res.* 118 (6), 1–18. doi:10.1002/jgre.20100

Dickson, J. L., Ehlmann, B., Kerber, L. A., and Fassett, C. I. (2024). The Global Context Camera (CTX) Mosaic of Mars: a product of information-preserving image data processing. *Earth and Space Science* 11 (7). doi:10.1029/2024EA003555

Draganits, E., and Janda, C. (2003). Subaqueous artesian springs and associated spring pits in a Himalayan pond. *Boreas* 32, 436–442. doi:10.1111/j.1502-3885.2003.tb01096.x

Edgett, K. S., and Sarkar, R. (2021). Recognition of sedimentary rock occurrences in satellite and aerial images of other worlds—insights from Mars. *Remote Sens.* 13 (21), 4296. doi:10.3390/rs13214296

Edwards, C. S., Bandfield, J. L., Christensen, P. R., and Fergason, R. L. (2009). Global distribution of bedrock exposures on Mars using THEMIS high-resolution thermal inertia. *J. Geophys. Res.* 114 (E11), 18. doi:10.1029/2009JE003363

Fairén, A. G. (2010). A cold and wet Mars. *Icarus* 208, 165–175. doi:10.1016/J.ICARUS.2010.01.006

Fassett, C. I., and Head, J. W. I. (2005). Fluvial sedimentary deposits on Mars: ancient deltas in a crater lake in the Nili Fossae region. *Geophys. Res. Lett.* 32 (L14201), 61–89. doi:10.1029/2005GL023456

Fassett, C. I., and Head, J. W. I. (2008). Valley network-fed, open-basin lakes on Mars: distribution and implications for Noachian surface and subsurface hydrology. *Icarus* 198, 37–56. doi:10.1016/j.icarus.2008.06.016

Fergason, R. L., Christensen, P. R., Kieffer, H. H., Golombek, M. P., and Herkenhoff, K. E. (2006). High-resolution thermal inertia derived from the thermal emission imaging system (THEMIS): thermal model and applications. *J. Geophys. Res.* 111 (E12004). doi:10.1029/2005JE002583

Gallagher, C. J., and Balme, M. R. (2015). Eskers in a complete, wet-based glacial system in the Phlegra Montes region, Mars. *Earth and Planetary Science Letters* 431. doi:10.1016/j.epsl.2015.09.023

Godt, J. W., and Coe, J. A., (2003). Map showing alpine debris flows triggered by a july 28, 1999 thunderstorm in the central front range of Colorado, USGS Open File Report 03-050.

Goldspiel, J. M., and Squyres, S. W. (1991). Ancient aqueous sedimentation on Mars. *Icarus* 89, 392–410. doi:10.1016/0019-1035(91)90186-W

Goudge, T. A., Milliken, R. E., Head, J. W., Mustard, J., and Fassett, C. I. (2017). Sedimentological evidence for a deltaic origin of the western fan deposit in Jezero crater, Mars and implications for future exploration. *Earth Planet. Sci. Lett.* 458, 357–365. doi:10.1016/j.epsl.2016.10.056

Grant, J. A., and Wilson, S. A. (2011). Late alluvial fan formation in southern Margaritifer Terra, Mars. *Geophys. Res. Lett.* 38 (L08201). doi:10.1029/2011GL046844

Grau Galofre, A., Howard, A. D., Morgan, A. M., Wilson, S. A., and Moore, J. M. (2024). Glacial sculpting of a martian cratered landscape on the northeastern flank of the Hellas basin. *Icarus* 420, 116211. doi:10.1016/j.icarus.2024.116211

Greeley, R. (1987). Release of juvenile water on Mars: estimated amounts and timing associated with volcanism. *Science* 236, 1653–1654. doi:10.1126/science.236.4809.1653

Guhman, A. I., and Pederson, D. T. (1992). Boiling sand springs, Dismal River, Nebraska: agents for formation of vertical cylindrical structures and geomorphic change. *Geology* 20 (1), 8–10. doi:10.1130/0091-7613(1992)020<0008:bssdrn>2.3.co;2

Gullikson, A. G., Anderson, R. B., and Williams, R. M. E. (2023). Spatial distribution and morphometry of sinuous ridges in southeastern Terra Sabea and the northern region of Hellas Planitia. *Icarus* 394, 14. doi:10.1016/j.icarus.2022.115399

Harvey, A. M. (1987). "Alluvial fan dissection: relationship between morphology and sedimentation," in *Desert sediments: ancient and modern*. Editors L. E. Frostick, and I. Reid (Oxford: Blackwell Scientific Publications), 87–103.

Harvey, A. M. (1997). "The role of alluvial fans in arid zone fluvial systems," in *Arid zone geomorphology: process, form and change in drylands*. Editor D. S. G. Thomas (Hoboken, N. J.: John Wiley), 109–129.

Harvey, A. M. (2003). "The response of dry-region alluvial fans to late Quaternary climatic change," in *Desertification in the third millennium*. Editors A. S. Alsharhan, W. W. Wood, A. S. Goudie, A. Fowler, and E. M. Abdellatie (Rotterdam: Balkema), 83–98.

Harvey, A. M., and Wells, S. G. (1994). "Late Pleistocene and Holocene changes in hillslope sediment supply to alluvial fan systems: zzyzz, California," in *Environmental change in drylands: biogeographical and geomorphological perspectives*. Editors A. C. Millington, and K. Pye (Chichester: Wiley), 67–84.

Harvey, A. M., and Wells, S. G. (2003). "Late Quaternary alluvial fan development, relations to climatic change, Soda Mountains, Mojave Desert, California," in *Environmental change in the Mojave Desert*. Editors N. Lancaster, Y. Enzel, and S. G. Wells (Boulder: Geological Society of America), 207–230.

Haug, E. W., Kraal, E. R., Sewall, J. O., Van Dijk, M., and Diaz, G. C. (2010). Climatic and geomorphic interactions on alluvial fans in the Atacama Desert, Chile. *Geomorphology* 121, 184–196. doi:10.1016/j.geomorph.2010.04.005

Head, J. W., and Marchant, D. R. (2014). The climate history of early Mars: insights from the Antarctic McMurdo Dry Valleys hydrologic system. *Antarct. Sci.* 26 (6), 774–800. doi:10.1017/S0954102014000686

Holo, S. J., Kite, E. S., Wilson, S. A., and Morgan, A. M. (2021). The timing of alluvial fan formation on Mars. *Planet. Sci. J.* 2 (210), 210. doi:10.3847/PSJ/AC25ED

Holzer, T. L., and Clark, M. M. (1993). Sand boils without earthquakes. *Geology* 21, 873–876. doi:10.1130/0091-7613(1993)021<0873:sbwe>2.3.co;2

Hynek, B. M. (2016). RESEARCH FOCUS: the great climate paradox of ancient Mars. *Geology* 44 (10), 879–880. doi:10.1130/focus102016.1

Hynek, B. M., Breach, M., and Hoke, M. R. T. (2010). Updated global map of Martian valley networks and implications for climate and hydrologic processes. *J. Geophys. Res.* 115, E09008. doi:10.1029/2009JE003548

Irwin, R. P., III, Howard, A. D., Craddock, R. A., and Moore, J. M. (2005). An intense terminal epoch of widespread fluvial activity on early Mars: 2. Increased runoff and paleolake development. *J. Geophys. Res.* 110 (E12). doi:10.1029/2005JE002460

Jaumann, R., Neukum, G., Behnke, T., Duxbury, T., Eichentopf, K., Flohrer, J., et al. (2007). The high-resolution stereo camera (HRSC) experiment on Mars Express: instrument aspects and experiment conduct from interplanetary cruise through the nominal mission. *Planet. Space Sci.* 55, 928–952. doi:10.1016/j.pss.2006.12.003

Kereszturi, A. (2012). Review of wet environment types on Mars with focus on duration and volumetric issues. *Astrobiology* 12 (6), 586–600. doi:10.1089/ast.2011.0686

Keske, A. L., Hamilton, C. W., McEwen, A. S., and Daubar, I. J. (2015). Episodes of fluvial and volcanic activity in Mangala Valles, Mars. *Icarus* 245, 333–347. doi:10.1016/j.icarus.2014.09.040

Kieffer, H. H., Martin, T. Z., Peterfreund, A. R., Jakosky, B. M., Miner, E. D., and Palluconi, F. D. (1977). Thermal and albedo mapping of Mars during the Viking primary mission. *J. Geophys. Res.* 82 (28), 4249–4291. doi:10.1029/JS082i028p04249

Kite, E., and Conway, S. J. (2024). Geological evidence for multiple climate transitions on Early Mars. *Nat. Geosci.* 17 (1), 10–19. doi:10.1038/s41561-023-01349-2

Kite, E. S., Sneed, J., Mayer, D. P., and Wilson, S. A. (2017). Persistent or repeated surface habitability on Mars during the late hesperian - amazonian. *Geophys. Res. Lett.* 44 (9), 3991–3999. doi:10.1002/2017GL072660

Kraal, E. R., Asphaug, E., Moore, J. M., Howard, A. D., and Bredt, A. (2008). Catalogue of large alluvial fans in martian impact craters. *Icarus* 194 (1), 101–110. doi:10.1016/j.icarus.2007.09.028

Lehmkuhl, F., and Owen, L. A. (2024). Alluvial fan types, distribution, and formation: a global perspective. *Z. für Geomorphol.* 64 (2), 95–142. doi:10.1127/zfg/2024/0826

Lehmkuhl, F., and Römer, W. (2022). Geomorphological processes and landforms in a global scale – previous concepts and future challenges from a German perspective. *Z. für Geomorphol.* 64, 53–71. doi:10.1127/zfg/2022/0767

Malin, M. C., and Edgett, K. S. (2000). Sedimentary rocks of early Mars. *Science* 290, 1927–1937. doi:10.1126/science.290.5498.1927

Malin, M. C., and Edgett, K. S. (2003). Evidence for persistent flow and aqueous sedimentation on early Mars. *Science* 302, 1931–1934. doi:10.1126/science.1090544

Malin, M. C., Edgett, K. S., Cantor, B. A., Caplinger, M. A., Calvin, W. M., Clancy, R. T., et al. (2007). Context camera investigation on board the Mars reconnaissance orbiter. *J. Geophys. Res.* 112 (EO5S04), 429–23,570. doi:10.1029/2006je002808

Mangold, N., Adeli, S., Conway, S., Ansan, V., and Langlais, B. (2012). A chronology of early Mars climatic evolution from impact crater degradation. *J. Geophys. Res.* 117 (E04003). doi:10.1029/2011JE004005

McEwen, A. S., Eliason, E. M., Bergstrom, J. W., Bridges, N. T., Hansen, C. J., Delamere, W. A., et al. (2007). Mars reconnaissance orbiter's high resolution imaging science experiment (HiRISE). *J. Geophys. Res.* 112 (E05S02). doi:10.1029/2005je002605

Miller, K., Simpson, E. L., Sherrod, L., Wizevich, M. C., Malenda, M., Morgano, K., et al. (2018). Gas bubble cavities in deltaic muds, Lake Powell delta, glen canyon national recreation area, hite, Utah. *Mar. Petroleum Geol.* 92, 904–912. doi:10.1016/j.marpetgeo.2018.03.032

Mondro, C. A., Moersch, J. E., and Hardgrove, C. (2024). Surface grain size of alluvial fans on Mars from thermal inertia, as an indicator of depositional style. *Icarus* 412, 115971. doi:10.1016/j.icarus.2024.115971

Moore, J. M., and Howard, A. D. (2005). Large alluvial fans on Mars. *J. Geophys. Res.* 110 (E04005). doi:10.1029/2004JE002352

Moore, J. M., Howard, A. D., Dietrich, W. E., and Schenk, P. M. (2003). Martian layered fluvial deposits: implications for Noachian climate scenarios. *Geophys. Res. Lett.* 30 (24), 2292. doi:10.1029/2003GL019002

Morgan, A. M., Howard, A. D., Hobley, D. E., Moore, J. M., Dietrich, W. E., Williams, R. M. E., et al. (2014). Sedimentology and climatic environment of alluvial fans in the martian Saheki crater and a comparison with terrestrial fans in the Atacama Desert. *Icarus* 229, 131–156. doi:10.1016/j.icarus.2013.11.007

Morgan, A. M., Wilson, S. A., and Howard, A. D. (2022). The global distribution and morphologic characteristics of fan-shaped sedimentary landforms on Mars. *Icarus* 385, 115137. doi:10.1016/j.icarus.2022.115137

Ramirez, R. M., and Craddock, R. A. (2018). The geological and climatological case for a warmer and wetter early Mars. *Nat. Geosci.* 11 (4), 230–237. doi:10.1038/s41561-018-0093-9

Ramsdale, J. D., Balme, M. R., Gallagher, C., Conway, S. J., Smith, I. B., Hauber, E., et al. (2018). Grid mapping the northern plains of Mars: geomorphological, radar, and water-equivalent hydrogen results from arcadia plantia. *J. Geophys. Res.* 124 (2), 504–527. doi:10.1029/2018JE005663

Ritter, B., Stuart, F. M., Binnie, S. A., Gerdes, A., Wennrich, V., and Dunai, T. J. (2018). Neogene fluvial landscape evolution in the hyperarid core of the Atacama Desert. *Sci. Rep.* 8 (1), 13952. doi:10.1038/s41598-018-32339-9

Sagan, C., Toon, O. B., and Gierasch, P. J. (1973). Climatic change on Mars. *Science* 181, 1045–1049. doi:10.1126/science.181.4104.1045

Salcher, B. C., Faber, R., and Wagreich, M. (2010). Climate as main factor controlling the sequence development of two Pleistocene alluvial fans in the Vienna Basin (eastern Austria) — a numerical modelling approach. *Geomorphology* 115, 215–227. doi:10.1016/j.geomorph.2009.06.030

Segura, T. L., McKay, C. P., and Toon, O. B. (2012). An impact-induced, stable, runaway climate on Mars. *Icarus* 220, 144–148. doi:10.1016/j.icarus.2012.04.013

Segura, T. L., Toon, O. B., Colaprete, A., and Zahnle, K. (2002). Environmental effects of large impacts on Mars. *Science* 298 (5600), 1977–1980. doi:10.1126/science.1073586

Shean, D. E., Fahle, J., Malin, M. C., Edwards, L. J., and Posiolova, L. (2011). MRO CTX stereo image processing and preliminary DEM quality assessment. *Lunar Planet. Sci. Conf.* Abstract #2646.

Sherrod, L., Simpson, E. L., Higgins, R., Miller, K., Morgano, K., Snyder, E., et al. (2016). Subsurface structure of water–gas escape features revealed by ground-penetrating radar and electrical resistivity tomography, Glen Canyon National Recreation Area, Lake Powell delta, Utah, USA. *Sediment. Geol.* 344, 160–174. doi:10.1016/j.sedgeo.2016.02.005

Stainstreet, I. G., and McCarthy, T. S. (1993). The Okavango Fan and the classification of subaerial fan systems. *Sediment. Geol.* 85, 115–133. doi:10.1016/0037-0738(93)90078-J

Stock, J. D. (2013). "Waters divided: a history of alluvial fan research and a view of its future," in *Treatise on geomorphology*. Editor J. E. W. Shroder (San Diego: Academic Press), 413–458.

Tanaka, K. L., Skinner, J. A., Dohm, J. M., Jr., Irwin, R. P., III, Kolb, E. J., Fortezzo, C. M., et al. (2014). *Geologic map of Mars*, 3292. U.S. Geological Survey Scientific Investigations Map, 43. doi:10.3133/sim3292

Ventra, D., and Clarke, L. A. (2018). Geology and geomorphology of alluvial and fluvial fans: current progress and research perspectives. *Special Publ. – Geol. Soc. Lond.* 440, 1–21. doi:10.1144/SP440.16

Williams, R. M. E., and Malin, M. C. (2008). Sub-kilometer fans in Mojave Crater, Mars. *Icarus* 98 (2). doi:10.1016/j.icarus.2008.07.013

Williams, R. M. E., Anderson, R. B., Gulikson, A. L., and Berman, D. C. (2024). *Data from: digital terrain models for Mars sinuous ridges and alluvial fans projects*. U.S. Geological Survey data release. doi:10.5066/P9I1QO1U

Wilson, A., Howard, A. D., Moore, J. M., and Grant, J. A. (2016). A cold-wet middle-latitude environment on Mars during the Hesperian-Amazonian transition: evidence from northern Arabia valleys and paleolakes. *J. Geophys. Res.* 121, 1667–1694. doi:10.1002/2016JE005052

Wilson, S. A., Morgan, A. M., Howard, A. D., and Grant, J. A. (2021). The global distribution of craters with alluvial fans and deltas on Mars. *Geophys. Res. Lett.* 48 (4). doi:10.1029/2020GL091653

Woor, S., Thomas, D. S. G., Parton, A., and Leenman, A. (2023). Morphology and controls of the mountain-front fan systems of the Hajar Mountains, south-east Arabia. *Earth-Science Rev.* 237 (104316), 104316. doi:10.1016/j.earscirev.2023.104316

Wordsworth, R. D. (2016). The climate of early Mars. *Annu. Rev. Earth Planet. Sci.* 44 (1), 381–408. doi:10.1146/annurev-earth-060115-012355

Wordsworth, R. D., Kerber, L., Pierrehumbert, R. T., Forget, F., and Head, J. W. (2015). Comparison of "warm and wet" and "cold and icy" scenarios for early Mars in a 3-D climate model. *J. Geophys. Res. Planets* 120 (6), 1201–1219. doi:10.1002/2015JE004787

Zaki, A. S., Pain, C. F., Edgett, K. S., and Castelltort, S. (2021). Global inventory of fluvial ridges on Earth and lessons applicable to Mars. *Earth-Science Rev.* 216 (1036561), 103561. doi:10.1016/j.earscirev.2021.103561

Zhang, M., Zhao, J., Xiao, L., Xy, Y., Bugiolacchi, R., and Want, J. (2023). Fan-shaped deposits in the northern Hellas region, Mars: implications for the evolution of water reservoir and climate. *Icarus* 395, 115470. doi:10.1016/j.icarus.2023.115470

Zuber, M. T., Smith, D. E., Solomon, S. C., Muhleman, D. O., Head, J. W., Garvin, J. B., et al. (1992). The Mars observer laser altimeter investigation. *J. Geophys. Res.* 97, 7781–7797. doi:10.1029/92JE00341